Environment International 120 (2018) 295–303

Contents lists available at ScienceDirect

Environment International

journal homepage: www.elsevier.com/locate/envint

In vitro inhalation bioaccessibility for particle-bound hydrophobic organic chemicals: Method development, effects of particle size and hydrophobicity, and risk assessment

Shan-Yi Xie, Jia-Yong Lao, Chen-Chou Wu, Lian-Jun Bao*, Eddy Y. Zeng

School of Environment and Guangdong Key Laboratory of Environmental Pollution and Health, Jinan University, Guangzhou 511443, China

ARTICLE INFO

Handling Editor: Adrian Covaci

Keywords:
Bioaccessibility
In vitro method
Polycyclic aromatic hydrocarbons
Size-fractionated particles
Human inhalation health risk

ABSTRACT

Bioaccessibility of particle-bound hydrophobic organic contaminants and related particle size effects are significant for assessing the potential human health risk *via* inhalation exposure, but have not been clearly evaluated. To fill this knowledge gap, the present study developed an *in vitro* method to estimate the inhalation bioaccessibility of particulate polycyclic aromatic hydrocarbons (PAHs) using simulated human lung fluids, *i.e.*, a modified Gamble's solution (MGS) and artificial lysosomal fluid (ALF) with Tenax as the absorption media. Assay parameters, namely incubation time (10 d) and influence of filter use, were optimized for establishing the *in vitro* method. The results showed that the bioaccessibility of PAHs increased with increasing particle size, but other factors, such as total organic carbon and chemical hydrophobicity, also played a large role in the fate of these compounds. The results from this portion of the present study were then used to evaluate human health risk, which showed that the risk of these particle-bound PAHs by incorporating size-dependent PAHs bioaccessibility and deposition efficiency in the human respiratory tract into inhalation exposure risk calculations was reduced by > 90% when compared to using total concentration. This suggested that the inhalation bioaccessibility and deposition efficiency of hydrophobic organic chemicals should be included in human health risk assessment.

1. Introduction

Air pollution has become one of the most important topics of research and governance in China over two decades (Beelen et al., 2014). Epidemiological studies have consistently shown that atmospheric particulate pollution increases the morbidity and mortality of exposed individuals due to respiratory diseases, *e.g.*, asthma, chronic obstructive pulmonary disease, and lung cancer (Balakrishnan et al., 2014; Beelen et al., 2014; Delfino et al., 2005; Zhang et al., 2017). Atmospheric particulate matter is a complex matrix of a variety of inorganic and organic compounds such as heavy metals and potentially a suite of organic contaminants (Choi et al., 2017; Kioumourtzoglou et al., 2015; Martins et al., 2016). Thus, in addition to the harmful effects of particulate matter itself, the harmful effects of contaminants absorbed on particulate matter cannot be overlooked.

However, not all contaminants can be completely released from particulate matter and absorbed into the bloodstream, as only a fraction of contaminants can release into interstitial fluids and an even smaller amount can pass through the cell membrane. Those that do, however, can accumulate in human organs and reach the body's circulatory system, resulting in risk to human health (Collins et al., 2015; Semple et al., 2004). The fractions which can dissolve in human interstitial fluids are defined as being bioaccessible, while those that can cross the cell membrane to enter into the capillaries and reach blood circulation are commonly referred to as being bioavailable (Collins et al., 2015; Semple et al., 2004). As assessments solely on total concentrations of toxic chemicals would greatly overestimate risk, researchers have gradually converted from using total concentration to using the bioaccessible and/or bioavailable fractions in risk assessments (Ruby and Lowney, 2012; Shen et al., 2016). The bioavailable fraction can be determined by evaluating the contents of toxic chemicals inside human blood or by exposures with animals (*e.g.*, mice, pigs, or monkeys), wherein concentrations can be evaluated in a variety of tissues (including blood, organs, *etc.*) (Cui et al., 2016; Kastury et al., 2017). Unfortunately, the use of human or animals as test subjects has limitations as sample collection can be difficult, expensive, and constrained by ethical concerns (Beriro et al., 2016). Thus, many researchers have chosen to evaluate the bioaccessible fraction, which can be obtained

* Corresponding author.
E-mail address: baolianjun@jnu.edu.cn (L.-J. Bao).

https://doi.org/10.1016/j.envint.2018.08.015
Received 27 May 2018; Received in revised form 29 July 2018; Accepted 6 August 2018
Available online 11 August 2018

through an *in vitro* simulation method rather than using the bioavailable fraction obtained through the more difficult *in vivo* method (Collins et al., 2015; Zhang et al., 2016).

To date, the *in vitro* methods for evaluating the inhalation bioaccessibility of heavy metals and hydrophobic organic chemicals (HOCs) varied with assay parameters such as simulated lung fluids and incubation times. Most researchers have adopted simulated lung fluids (such as Gamble solution (GS) and artificial lysosomal fluid (ALF)) (Li et al., 2015; Wiseman and Zereini, 2014; Witt et al., 2014; Zereini et al., 2012). The GS simulates extracellular interstitial fluid within the deep lung (at a pH of 7.4–7.6), while the ALF mimics the intracellular fluid of alveolar and macrophages after phagocytosis of particulate matter (at a pH of 4.5–5.0) (Pelfrêne et al., 2017; Wiseman, 2015). Although some researchers have used unmodified GS, other researchers have also started modifying the GS to mimics the pulmonary environment more closely (Boisa et al., 2014; Julien et al., 2011). Previous studies found that the epithelial type II cells secrete lung surfactant, which is highly enriched with dipalmitoyl-sn-glycero-3-phosphocholine (DPPC), into the alveolar space to lower the surface tension at the air-liquid interface (Bernhard, 2016; Veldhuizen and Haagsman, 2000). Thereby, one commonly used modification is the addition of DPPC. This surfactant has been shown to significantly increase the bioaccessibility of Pb by 5.6% to 18% (Li et al., 2016), and its use is considered to be more biologically relevant (and as such was used in the present study as well).

However, the simulated lung fluids such as GS or ALF have largely been used to assess the bioaccessibility of heavy metals on particulate pollutants (Dartey et al., 2014; Wiseman, 2015), with little information regarding inhalation bioaccessibility of organic pollutants (Wei et al., 2018). A recent review (Wei et al., 2018) found only five articles on measuring the bioaccessible fractions of HOCs using *in vitro* methods. Different artificial lung fluids (water, phospholipid vesicles, 1-octanol, and saline containing DPPC) (Bevan and Yonda, 1985; Borm et al., 2005; Gerde et al., 2001) were used and these *in vitro* methods were developed without carefully examining the effects of bioassay parameters, such as incubation time and temperature. Although Kademoglou et al. (2018) recently applied the GS and ALF to evaluate the inhalation bioaccessibility of phthalate esters and alternative plasticizers in indoor dusts, they also pointed out the necessity to develop a unified and biologically relevant *in vitro* method for inhalation bioaccessibility. In addition, particulate matter ranges over four orders of magnitude in diameter, from nanometers to microns. The effects of particle size and chemical hydrophobicity on inhalation bioaccessibility of HOCs remain limited, even unknown. Therefore, the need for research in this area is highly warranted.

The objectives of the present study were to (1) develop an *in vitro* method using sediment particles in modified GS or ALF, optimizing for incubation time and evaluating the effects of filter use; (2) examine the effects of particle size and hydrophobicity on inhalation bioaccessibility of particle-bound polycyclic aromatic hydrocarbons (PAHs); and (3) assess the associated health risks based on total concentration, deposition efficiency, and a combination of deposition efficiency and inhalation bioaccessible fraction of PAHs with e-waste burning particles as a case study.

2. Materials and methods

2.1. Materials and method optimization – sample preparation

Twenty-five individual PAHs (including BP, 2,6-DNAP, AC, ACE, 2,3,5-TNAP, FL, PHE, ANT, 2-MPHE, 1-MPHE, 2,6-DMPHE, FLU, PYR, 11-BbF, BaA, CHR, B[b]F, B[k]F, BeP, BaP, PER, 9,10-DPHA, IcdP, DahA, and BghiP) were selected as target compounds. The physical-chemical properties and full names of individual PAHs, and detailed purity of standards and reagents are presented in Table S1 and Text S1 of Supplementary data; "S" designates text, tables, and figures in the Supplementary data afterwards.

Before e-waste burning particle samples could be evaluated, the *in vitro* method needed to be optimized for both fluids being used (*i.e.*, to evaluate incubation time and to determine if filter use would affect bioaccessibility) by using spiked sediment particles. Sediment samples were collected from Dongjiang River in Dongguan, Guangdong Province, China with a stainless steel grab. The sediment was dried at 60 °C in an oven, ground with a mortar and pestle, and sieved through 187 μm sieve to obtain sediment particle samples. Sediment particles (aerodynamic diameter: 5.9 ± 5.0 μm; Zeiss Microscopy) were then spiked with a mixture of the target PAHs in 5 mL dichloromethane for 20 mg of particles to achieve individual PAH concentrations of 10 μg g^{-1}. Spiked sediment samples were aged for one month before use. Prior to each incubation, the concentrations of spiked sediment PAHs were confirmed analytically. In short, 20 mg of the spiked sediment was placed into a Teflon tube, spiked with the surrogate standards (0.1 μg) in hexane, and sonicated three times (30 min each) with a mixed solvent of hexane, dichloromethane, and acetone (2:2:1 in volume). These three extracts were combined, solvent-exchanged to hexane, and concentrated to 1 mL under a gentle stream of N_2. The extract was purified on a glass column packed with neutral silica gel (12 cm) and anhydrous sodium sulfate granular (1 cm) from bottom to top, and again concentrated to 0.1 mL under N_2. All samples were spiked with the internal standards (0.1 μg) before instrumental analysis.

Although the sediment particles were not completely representative of inhaled particles, they were comparable surrogates for developing the *in vitro* method as the effects of assay parameters on the releases of HOCs from sediment and inhaled particles into lung fluids were deemed similar.

2.2. Method optimization – bioaccessibility experiments

Bioaccessibility assays were undertaken to evaluate incubation time and filter use with both artificial lung fluids (ALF and GS). Only the GS was modified (referred to as MGS afterwards) by adding 100 mg of DPPC into every 1000 mL of the original GS. The final chemical compositions of ALF (pH = 4.5) without bio-surfactant and MGS (pH = 7.4) are presented in Table S2. Prior to experiments, Tenax (1 g) was wrapped with two layers of metallic sieve (mesh size of 13 μm) and stainless steel wire to produce a small 'stick-like' structure (Fig. S1) wherein both ends were blocked with a Teflon plug. The small 'stick-like' structure looks like a column with the radius of 1 cm and length of 10 cm. This Tenax, 200 mL of either ALF or MGS, and 20 mg of spiked particulate sample were mixed in a glass bottle, incubated at 37 °C, and shaken at 150 rpm for 0.5, 1, 2, 3, 7, 10, and 14 d. Although the total human lung fluid volume is around 20–60 mL, the solid/liquid ratio (1/10000; g/mL) was taken account into the mass of particle matter deposited in the lung and volume of lung liquid (Kastury et al., 2017). Another mixture was prepared using the same amounts and procedure to evaluate the role of the 47 mm diameter glass microfiber filter (Whatman International, Maidstone, England). The filter was added at the same time as the Tenax, and the mixture was allowed to incubate for 10 d. Additionally, there was one more mixture without Tenax and glass microfiber filter to incubate for 3 d. At each time point, Tenax was carefully removed, rinsed thoroughly with deionized water, and placed in a Teflon tube. All rinsing waters were also collected and combined with leftover simulated lung fluid solution (referred to as 'simulated lung fluid' solution moving forward) and filtered through a mixing fibroid membrane (0.2 μm) to separate particles from the solution. This solution and the particles obtained from filtering were kept for future chemical analysis. Five replicates were performed during each bioaccessibility assay.

All samples were spiked with the surrogate standards before extraction. 'Simulated lung fluid' solution (approximately 230 mL) was liquid-liquid extracted three times, each with 40 mL of dichloromethane in a 1000-mL separatory funnel. The Tenax insert was

sonicated three times (30 min each) with 25 mL of a mixture of hexane and acetone (1:1 in volume). Particulate matter was sonicated three times, each with 15 mL of a mixture of hexane, dichloromethane, and acetone (2:2:1 in volume). All extracts were dried with anhydrous sodium sulfate, concentrated (using N_2), solvent-exchanged to hexane, and concentrated again to 1 mL. Each of these was purified on a glass column packed with neutral silica gel (5 cm for 'simulated lung fluid' solution and 12 cm for Tenax and particulate residues) and anhydrous sodium sulfate (1 cm for all samples) from bottom to top. Samples were concentrated to 0.1 mL under N_2, and finally spiked with internal standards (50 ng for 'simulated lung fluid' samples and 100 ng for particulate and Tenax samples) before instrumental analysis. The procedures and parameters of instrumental analysis are detailed in Text S1.

2.3. Effects of particle size experiments

To represent open-burned e-waste, a TV casing (front) was collected from an e-waste collection factory in Foshan, Guangdong Province, China. The TV casing was crushed and sieved to yield fractions between 840 μm to 2000 μm. A 2-g sample of this crushed matter was burned with a spray gun for 5 min within a stainless steel rectangular box (0.5 × 0.5 × 1.5 m). The air being introduced into the box (during collection of particles) was cleaned with a glass microfiber filter and a polyurethane foam. Size-fractionated airborne particle samples were collected with a Micro-Orifice Uniform Deposit Impactor (M110-R, MSP Corporation, Shoreview, MN, USA) during a 3-h sampling period. All particulate samples were collected on 47 mm diameter glass microfiber filters at a flow rate of 30 L min^{-1}, and separated initially into 11 size fractions (from 0.056 to larger than 18.0 μm). However, as some fractions contained non-detectable target analytes (Fig. S2), the number of fractions evaluated was reduced to six (0.056–0.18, 0.18–0.32, 0.32–0.56, 0.56–1.0, 1.0–1.8, and 1.8–5.6 μm), each of which was extracted with the optimized procedures discussed above. Three replicates were conducted for open-burned e-waste. All airborne particle samples were incubated in ALF or MGS with Tenax for 10 d. In addition, total organic carbon (TOC) in each airborne e-waste particle sample was measured with an elemental analyzer (Vario EI III Elementar, Element, Germany), which are detailed in Text S1.

2.4. Quality assurance and quality control

One procedural blank with solvents only or glass microfiber filter without particles was analyzed with every 10 samples and concentrations of detected target analytes had blank samples concentrations deducted. The recoveries of the surrogate standards, *i.e.*, naphthalene-d_8, acenaphthene-d_{10}, phenanthrene-d_{10}, chrysene-d_{12}, perylene-d_{12}, and benzo[*ghi*]perylene-d_{12}, were 71 ± 13%, 76 ± 14%, 89 ± 17%, 92 ± 17%, 82 ± 20%, and 85 ± 17% in extracted liquid samples, 69 ± 11%, 73 ± 18%, 71 ± 16%, 82 ± 20%, 82 ± 23, and 83 ± 21% in extracted Tenax samples, 64 ± 9%, 69 ± 11%, 73 ± 10%, 87 ± 14%, 82 ± 17%, and 80 ± 15% in particle samples after incubation, and 73 ± 15%, 80 ± 15%, 81 ± 14%, 99 ± 17%, 101 ± 21%, and 103 ± 20% in particle samples. The sum of the masses of PAHs in Tenax, artificial lung fluid, and residual particulates was 99 ± 24% of the initial mass. The lowest calibration concentration divided by the actual sample volume/weight was defined as the reporting limit for a target compound, which was 0.09 ng m^{-3} for each of PAHs evaluated for the e-waste burning particle samples.

2.5. Data analysis

Inhalation bioaccessibility fraction (IBAF; %) was the chosen endpoint in the present study and is defined as:

$$\mathrm{IBAF} = \frac{M_Y + TA}{M_Y + TA + M_P} \times 100\% \quad (1)$$

where M_Y refers to the mass of the target compound released into the simulated lung fluid; M_P is the residual fraction in the e-waste airborne particle or spiked sediment particle of the target compound after incubation; and TA is the mass of the target compound absorbed onto the Tenax. The calculated IBAF was used to evaluate the potential inhalation health risk from open e-waste burning, with the use of $Risk_O$, $Risk_{DE}$, and $Risk_{DE+BA}$, which are defined as the inhalation health risk based on the total concentration of contaminant, the deposited fraction in the lung, and the deposited fraction that can dissolve into lung fluid (or bioaccessible fraction), respectively. As such, the overall concentration and therefore the risk are refined with each step, with $Risk_{DE+BA}$ providing the most accurate assessment. It should be noted that the relative potential inhalation health risks with different estimated methods were assessed and have not been compared with the actual exposure risk. The health risk assessed in the present study is calculated based on concentrations of PAHs in the e-waste airborne particles (Table S3), with the procedures detailed in Text S2.

3. Results and discussion

3.1. Method development

When inhaled particle-bound HOCs enter into the human lungs, complex physiological processes, including a continuous sorption of HOCs from the lung fluids to maintain a concentration gradient between particles and fluids, occur in human body. Although other physiological activities would not be easy to identify, the sorption of HOCs in the human lungs could be mimicked with inclusion of a sorption sink to avoid underestimating the bioaccessibility of HOCs, similar to the *in vitro* digestive models. Tenax, a porous polymer resin, has been widely used in various *in vitro* studies to measure bioaccessibility of HOCs (Cui et al., 2016; Fang and Stapleton, 2014). In addition, Fang and Stapleton (2014) found that the oral bioaccessibility of PBDEs in house dust Reference Standard Material (SRM) 2385 in the digestive fluids with Tenax as the sink were comparable with those net absorption rates in the *in vivo* study using Sprague−Dawley rats dosed with SRM 2585. Furthermore, the IBAF values of PAHs, especially higher-ring PAHs, in two simulated lung fluids with Tenax were greater than the values without Tenax (Fig. 1). Therefore, Tenax was selected as a sorption sink to simulate the sorption of PAHs in the human lung environment in the present study.

One of the principal ideas of the *in vitro* method is that it should simulate the retention of particulate matter in the respiratory tract. As retention reflects the combined effect of deposition and clearance velocity, it is dependent on the particle diameters, deposition patterns, and characteristics of an organism's bronchial airway (Hofmann and Asgharian, 2003). Hofmann and Asgharian (2003) found that 10% to 15% of the initially deposited particles in human bronchial tree cannot be cleared *via* the lung mucus even 24 h after deposition. In fact, clearance of some fine inhaled particles from the alveoli region can take a considerably long time to complete, ranging from several days to several years (Twining et al., 2005). Numerous factors, most of which are difficult to quantify, can affect the retention of target compounds (such as immune response within an organism, characteristics of the compounds themselves, *etc.* (Kastury et al., 2017)) and ultimately equilibrium of these compounds in the lung. Because the time required for most particle-bound HOCs, including PAHs, to reach equilibrium with artificial lung fluids within the respiratory tract remained unknown, the first objective of the present study was to evaluate the changes of IBAF under different incubation times in each of the simulated lung fluids.

The IBAFs of most individual PAHs increased rapidly with incubation time in both ALF and MGS. The equilibrium time of PAHs increased with increasing number of benzene rings in both solutions. However, individual PAHs reached equilibrium at various incubation times, which also differed between the lung fluids evaluated (Figs. 2 and

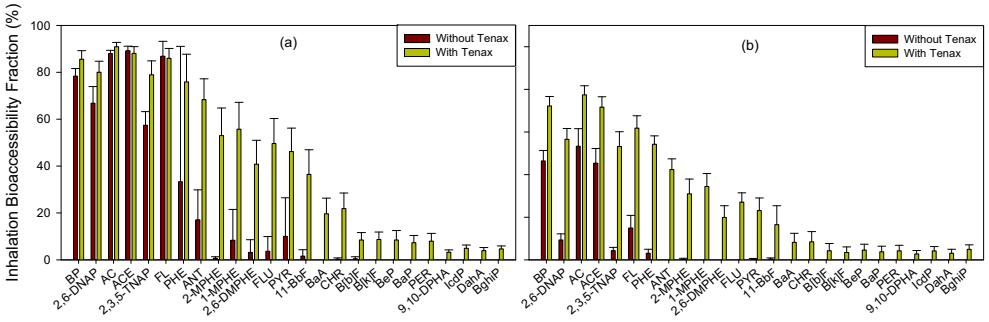

Fig. 1. Inhalation bioaccessibility fraction (IBAF; %) for PAHs during incubation with Tenax and those without in both artificial lysosomal fluid (ALF; a) and modified Gamble solution (MGS; b).

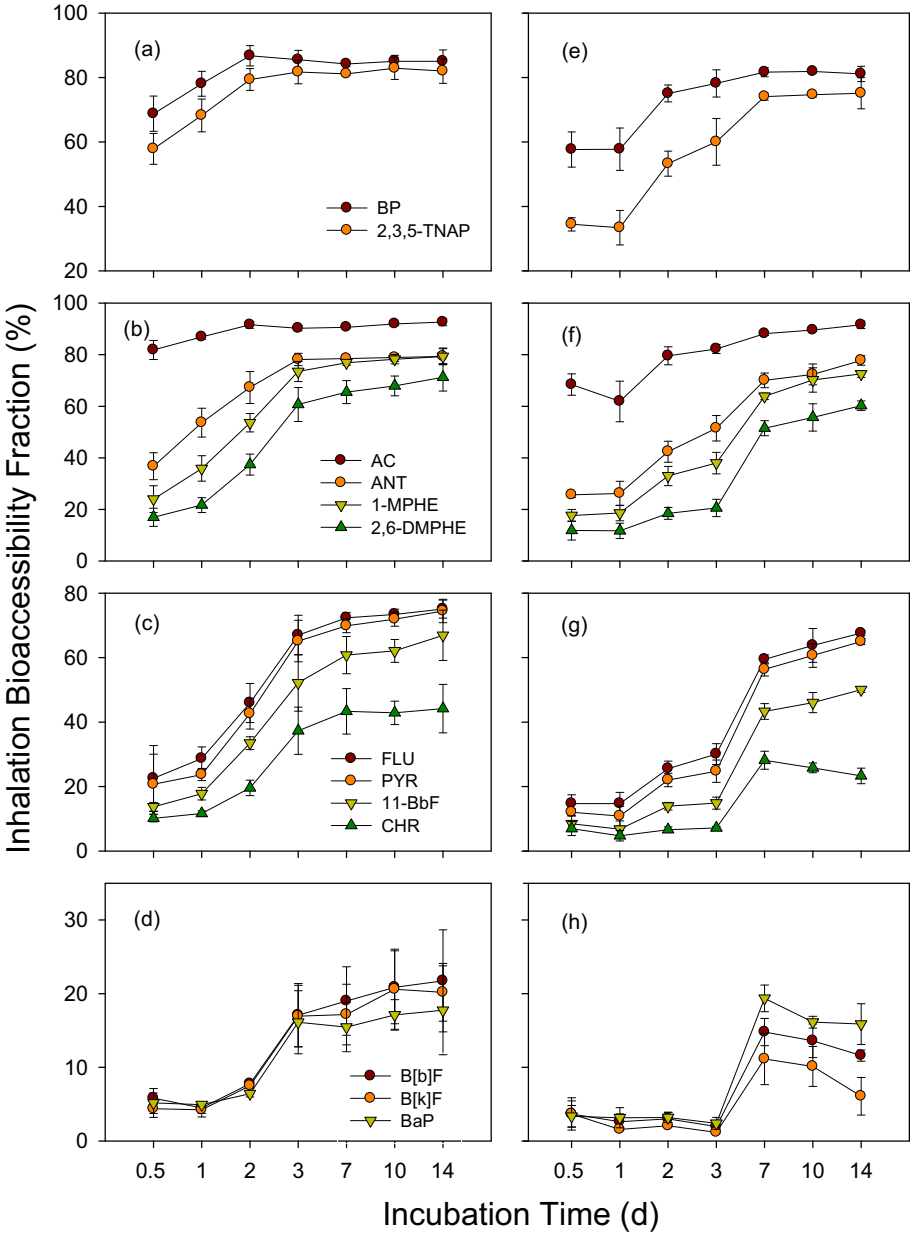

Fig. 2. Inhalation bioaccessibility fraction (IBAF) of a subset of PAHs analyzed after various incubation times in artificial lysosomal fluid (ALF; a–d) and in modified Gamble solution (MGS; e–h). Figs. (a) and (e) are 2-ring PAHs, (b) and (f) are 3-ring PAHs, (c) and (g) are 4-ring PAHs, and (d) and (h) are 5-ring PAHs. Additional results can be found in Figs. S3 and S4.

S3–S4). For instance, 2-ring PAHs approached equilibrium within 3 d in ALF, while 3-ring and 4 to higher-ring PAHs required 7 d and between 7 and 10 d, respectively. These same target PAHs, especially those with fewer rings, required more time to reach equilibrium in MGS, as 2-ring PAHs approached equilibrium within 7 d, while 3-ring and 4 to higher-ring PAHs required 10 d. However, no significant differences between IBAFs of individual PAHs (for each individual fluid) were noted between 10 and 14 d (independent-samples *t*-test, $p > 0.05$). As a result, a 10-d incubation time was chosen for all future work.

Another hindrance with the development of an *in vitro* method was the need of filter materials for the collection of air particles. In reality, particles enter the human respiratory system and make contact directly with pulmonary fluids, but in the routine experiments particles would first need to be loaded onto a glass microfiber membrane (*via* air samplers). During the sampling process some particles were more deeply embedded than those in the glass microfiber membranes, and as such not all particles could be entirely removed from the membrane material. Therefore it was important to evaluate the use of these glass microfiber filters on IBAF before a reliable *in vitro* method could be established.

The results of the 10-d incubation experiment using both simulated lung fluids were also used to evaluate the presence and absence of glass fiber filters. This portion of the present study revealed no significant differences of IBAFs of the target analytes (with the exception of 2,3,5-TNAP in MGS; Fig. 3) between the presence and absence of filters. These results suggested that the use of glass microfiber filters to collect field samples would not affect the outcome of the *in vitro* method.

Outside of validating the incubation time as well as the use of filters, it was also important to maintain mass balance in the system. The absolute recovery of 10-d incubated samples, which was the sum of the PAH masses in Tenax, artificial lung fluid, and residual particle divided by the initial mass, ranged from 92% to 112% and 75% to 99% for ALF and MGS, respectively (Table S4). With mass balance achieved in the test system and incubation time and filter use optimized, e-waste burning particle samples could be analyzed with confidence.

3.2. Bioaccessibility of PAHs in e-waste particles in ALF and MGS lung solutions

The IBAF values were quite different between the two lung solutions, and greater significantly in ALF for 4-ring PAHs (AVOVA, $p < 0.05$) (which was similar to the sediment particle results). For instance, IBAF values of 4-ring PAHs were all above 60% (regardless of particle size) in ALF, but were in most circumstances below 50% in MGS (Table 1). However, Kademoglou et al. (2018) found that there were no statistically significant differences for IBAF values of phthalates and alternative plasticizers (except dimethyl phthalate) in the two simulated lung fluids (ALF and GS without DPPC). In addition, the apparent bioaccessibility of most PAHs during the small intestine stage increased with increasing pH values due to the reduction in the aggregation number of dihydroxy bile acid micelles (Zhang et al., 2015). In the present study, MGS-containing DPPC is neutral (pH = 7), while ALF is more acidic (pH = 4). The DPPC contains a hydrophilic side with a negative charge on the phosphate group and a positive charge on the choline group. The differences on IBAF values of PAHs between the two simulation fluids may be attributed to the formation of DPPC micelle concentrations in MGS, which may affect the bioaccessibility of low hydrophobicity PAHs and needs to be further investigated. These results suggest that different lung solutions may behave differently and result in different estimates of risk. The results from the present study also indicate that PAHs may uptake more in the intracellular lung environment (as represented by ALF), rather than *via* the extracellular matrix (as represented by MGS). However, this should not be interpreted as one simulation solution being better than the other, as the solutions provide information for different parts of the lung, and for that reason, if possible, both simulated lung fluids should be evaluated in future studies.

Although the IBAFs were higher in ALF than in MGS, many trends were similar between the two fluids. The first trend is that in both solutions, only a subset of PAHs were detected at high concentrations for accurate quantification. Concentrations of 2- and 3-ring PAHs were too low to accurately quantify IBAF and as such were not evaluated further in this portion of the present study. The reason for this was most likely due to the tendency of lower-ring PAHs to partition more easily to the gas phase than to the particulate phase (Zhang et al., 2012). Another interesting finding was that PER and IcdP were not detected in MGS, but were detected in ALF. It may be due to the smaller amount of particles used in MGS than ALF (Table 1) and requires further investigation.

3.3. Role of hydrophobicity

Another trend that was similar for both solutions was that IBAFs were higher for lower-ring PAHs (*i.e.*, 4-ring > 5-ring > 6-ring) (independent-samples *t*-test, $p < 0.05$; Table 1). This trend was also apparent in the spiked sediment particles. As the lower-ring PAHs are more hydrophilic than the higher-ring ones, this result was not surprising, as the ability of chemicals to transit from particles to interstitial fluid is highly dependent on hydrophobicity (Collins et al., 2015; Fang and Stapleton, 2014; McLachlan, 1994). The PAHs in the present study have a wide range of log K_{OW} values (from 4.02 to 6.70), and their IBAF values, following a sigmoidal distribution, decreased with increasing hydrophobicity (or higher log K_{OW} values) for e-waste burning particles (Figs. 4 and 5). The coefficients of determination (R^2) for the IBAF and log K_{OW} correlations ranged from 0.50 to 0.93 in ALF and 0.46 to 0.83 in MGS. These R^2 values are quite high, especially considering that these correlations include all differing size fractions, showing the importance of hydrophobicity in assessing inhalation health risk.

These same trends have been reported by other researchers as well, *e.g.*, Fang and Stapleton (2014) showed similar results in flame

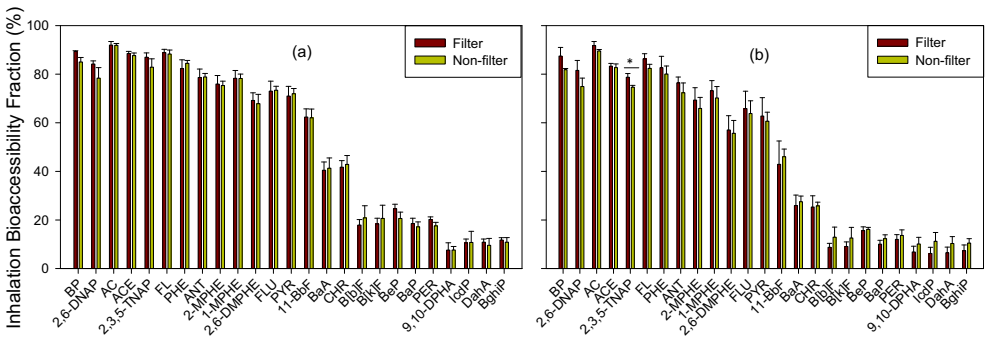

Fig. 3. Comparing inhalation bioaccessibility fraction (IBAF; %) for PAHs on sediment particles processed during incubation with and without a glass fiber filter in both artificial lysosomal fluid (ALF; a) and modified Gamble solution (MGS; b). The symbol "*" represents the significant level ($p < 0.05$) between groups.

Table 1
Inhalation bioaccessibility fraction (average ± standard deviation; %) of polycyclic aromatic hydrocarbons in burned e-waste samples as a function of particle diameter (μm) in artificial lysosomal fluid (ALF) and modified Gamble solution (MGS). In the ALF and MGS solution, 13 and 11 PAHs, respectively, were detected out of 25 evaluated.

Fluid solution	Cyclic rings	PAH name	Size fraction (μm)					
			0.056–0.18	0.18–0.32	0.32–0.56	0.56–1.0	1.0–1.8	1.8–5.6
% TOC			31	35	38	30	33	33
Particle mass (mg)			1.47	1.85	3.89	2.89	1.59	1.71
ALF	4	FLU	93.0 ± 1.4^{a}	95.0 ± 1.8^{a}	89.6 ± 3.8^{a}	94.8 ± 2.7^{a}	92.4 ± 0.5^{a}	92.4 ± 3.4^{a}
		PYR	93.7 ± 1.4^{ac}	96.1 ± 1.5^{ab}	91.1 ± 3.2^{ac}	96.8 ± 0.5^{b}	92.8 ± 0.7^{c}	87.9 ± 13.0^{abc}
		11-BbF	87.5 ± 3.2^{a}	90.1 ± 3.3^{a}	79.9 ± 9.3^{a}	89.2 ± 6.6^{a}	91.9 ± 4.3^{a}	93.9 ± 5.5^{a}
		BaA	61.8 ± 11.8^{ab}	66.2 ± 7.7^{ab}	50.3 ± 15.6^{a}	73.0 ± 13.4^{bcd}	84.6 ± 7.1^{cd}	83.5 ± 3.3^{d}
		CHR	63.4 ± 11.76^{ab}	69.6 ± 6.8^{ab}	52.7 ± 14.7^{a}	76.1 ± 13.4^{bcd}	86.3 ± 5.7^{cd}	85.7 ± 3.5^{d}
	5	B[b]F	20.7 ± 6.8^{ab}	26.6 ± 2.3^{ab}	15.6 ± 7.4^{a}	37.7 ± 16.1^{bcd}	56.3 ± 12.7^{cd}	61.33 ± 11.4^{d}
		B[k]F	18.2 ± 6.3^{ab}	25.8 ± 3.2^{ab}	15.0 ± 8.3^{a}	32.6 ± 13.1^{bcd}	53.7 ± 14.0^{cd}	57.1 ± 9.3^{d}
		BeP	21.6 ± 6.8^{ab}	26.0 ± 2.7^{ab}	16.4 ± 6.8^{a}	36.1 ± 15.0^{bcd}	56.5 ± 13.4^{cd}	59.3 ± 8.8^{d}
		BaP	20.0 ± 7.1^{ab}	25.6 ± 3.4^{ab}	14.4 ± 7.0^{a}	33.3 ± 14.6^{bcd}	45.6 ± 9.4^{cd}	50.7 ± 12.8^{d}
		PER	19.6 ± 6.8^{ab}	25.8 ± 3.5^{ab}	15.9 ± 6.3^{a}	50.7 ± 42.8^{b}	66.9 ± 29.4^{abc}	68.7 ± 27.5^{c}
		DahA	5.4 ± 2.6^{ab}	9.0 ± 4.5^{ab}	3.7 ± 1.3^{a}	12.4 ± 8.1^{ab}	28.4 ± 16.3^{ab}	22.4 ± 11.0^{b}
	6	IcdP	6.5 ± 2.5^{a}	10.2 ± 4.0^{a}	4.1 ± 2.5^{a}	13.7 ± 8.4^{ab}	34.9 ± 24.0^{ab}	25.4 ± 8.2^{b}
		BghiP	2.8 ± 2.8^{a}	6.1 ± 2.4^{a}	4.3 ± 2.3^{a}	6.6 ± 3.1^{ab}	25.6 ± 18^{ab}	17.2 ± 5.4^{b}
% TOC			33	43	45	46	41	48
Particle mass (mg)			0.77	1.11	1.24	0.89	0.64	0.63
MGS	4	FLU	54.7 ± 8.8^{a}	62.1 ± 6.0^{ab}	63.1 ± 13.0^{ab}	60.0 ± 8.8^{ab}	72.2 ± 5.7^{b}	75.4 ± 6.8^{b}
		PYR	52.6 ± 7.2^{a}	61.0 ± 5.8^{ab}	59.5 ± 15.7^{ab}	56.0 ± 8.3^{ab}	73.5 ± 7.1^{b}	77.5 ± 12.7^{b}
		11-BbF	42.2 ± 9.6^{a}	49.2 ± 8.9^{abc}	50.0 ± 15.0^{abc}	44.8 ± 8.4^{ab}	63.9 ± 9.3^{b}	67.6 ± 10.0^{c}
		BaA	12.3 ± 4.0^{a}	16.0 ± 6.4^{ab}	15.6 ± 8.3^{ab}	12.7 ± 4.1^{a}	30.7 ± 8.2^{b}	34.4 ± 11.0^{c}
		CHR	17.2 ± 4.0^{a}	21.9 ± 7.0^{abc}	17.3 ± 8.7^{a}	13.6 ± 4.3^{a}	38.0 ± 9.2^{b}	40.6 ± 11.4^{c}
	5	B[b]F	6.1 ± 1.6^{a}	9.7 ± 6.2^{ab}	5.7 ± 3.1^{a}	5.7 ± 3.1^{a}	16.9 ± 2.6^{b}	23.9 ± 17.6^{ab}
		B[k]F	5.8 ± 2.9^{a}	9.1 ± 6.6^{ab}	4.4 ± 2.5^{a}	5.0 ± 3.0^{a}	16.0 ± 4.7^{b}	26.3 ± 17.9^{ab}
		BeP	4.3 ± 0.7^{ac}	6.9 ± 2.0^{ab}	5.4 ± 3.6^{ab}	3.0 ± 3.3^{a}	13.4 ± 5.2^{bc}	19.7 ± 9.3^{c}
		BaP	8.8 ± 3.5^{ac}	12.1 ± 4.4^{ab}	7.2 ± 4.2^{ab}	5.1 ± 6.1^{a}	21.8 ± 6.7^{bc}	44.7 ± 32.3^{c}
		DahA	3.1 ± 3.0^{a}	6.9 ± 4.1^{ab}	4.5 ± 2.8^{ab}	4.7 ± 3.1^{ab}	13.0 ± 5.4^{bc}	20.9 ± 3.9^{c}
	6	BghiP	5.8 ± 2.4^{a}	8.0 ± 3.3^{a}	4.0 ± 2.2^{a}	10.6 ± 10.0^{ab}	16.0 ± 8.7^{ab}	26.3 ± 7.0

Different superscript letters indicate the significant differences between groups ($p < 0.05$).

retardants found in dust samples in the digestive system, as bioaccessibility decreased in a sigmoidal distribution with increasing hydrophobicity. Kademoglou et al. (2018) found that the IBAF of phthalate esters and alternative plasticisers in indoor dusts and SRM 2585 decreased with increasing hydrophobicity. To explain this relationship, McLachlan (1994) proposed a two-way resistance model, *i.e.*, two films, a water and an organic film, control the absorption in the digestive tract, but act differently in the organism and are both highly dependent on the properties of the contaminant. The organic film is the dominant 'resistor' for adsorption when K_{OW} is small and behaves independently of log K_{OW}. However, the water film becomes the primary 'resistor' of adsorption when log K_{OW} is high, and this film is highly depend on the log K_{OW} of the compound. Thus in theory, the diffusive transport of chemicals with high log K_{OW} values (such as a large number of PAHs in the present study) through the water barrier is quite low, resulting in low IBAFs for these compounds. The results from the present study also suggest that this two-way resistance model may occur in the lungs as well.

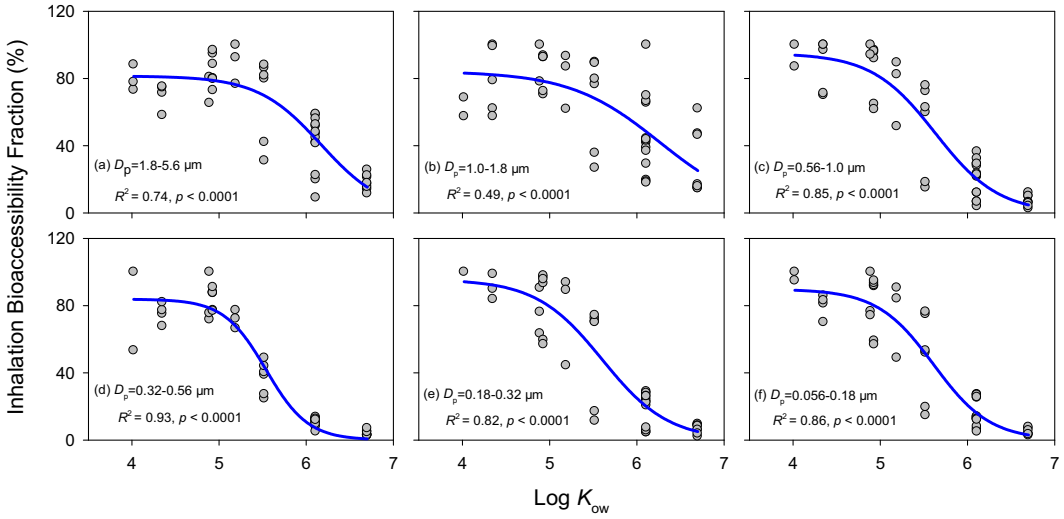

Fig. 4. Relationship between inhalation bioaccessibility fraction of PAHs present on various sizes of e-waste burning particle matter and their associated log K_{OW} values in artificial lysosomal fluid (ALF). Dp is the aerodynamic diameter of particle.

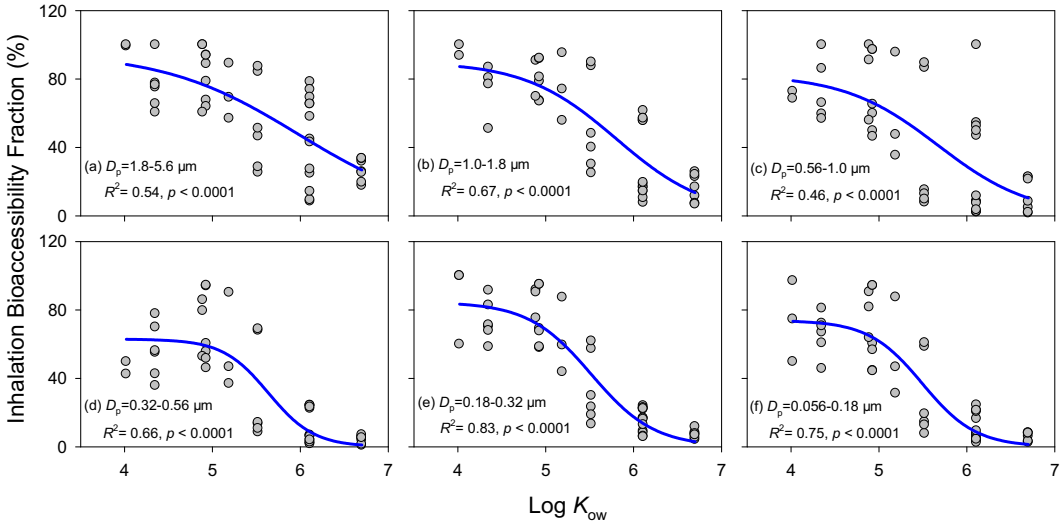

Fig. 5. Relationship between inhalation bioaccessibility fraction of PAHs present on various sizes of e-waste burning particle matter and their associated log K_{OW} values in modified Gamble solution (MGS). Dp is the aerodynamic diameter of particle.

3.4. Particle size effects

Another similar trend between the two solutions was that IBAFs of PAHs increased with increasing particle size, with one exception (Table 1). The exception is the insignificant difference of IBAFs for most 4-ring PAHs between some size fractions in ALF (AVOVA, $p > 0.05$). It is most likely that these compounds completely dissolve in ALF rapidly, with particle size exerting little influence on bioaccessibility. Outside of this one exception, IBAFs were consistently higher in large size fractions, up to 9.1 and 8.7 folds from the smallest to the largest fraction for ALF and MGS, respectively. These results were expected as many studies have shown that finer particles contain greater surface areas allowing for stronger sorption of chemicals onto organic matter (Cornelissen et al., 1997; Mehler et al., 2011; Sun et al., 2008).

Interestingly, previous studies using more traditional fluids (deionized water, acetate buffer, and nitric acid) have shown that particle size effects may be contaminant class specific, as some metals seem to behave differently than PAHs in the present study. For instance, Birmili et al. (2006) found that some heavy metals (Pb, Co, and Cd) in air particulate matter, using water as the exposure media, have high solubility in the fine particle size range, whereas other metals (Zn and Ba) showed the opposite trend. They speculated that finer particles containing Pb, Co, and Cd originated from high-temperature combustion sources which emit a higher fraction of water-soluble particles than coarse particles resulting in a more soluble ion phase in this fraction. Another study evaluated the association of the properties of Cu with different size fractions of airborne particulate matter in two exposure medias, acetate buffer and nitric acid. Copper bioaccessibility was different dependent on which solution was used, *i.e.*, increased bioaccessibility was noted with increasing particle size for nitric acid, but no correlation was found between bioaccessibility and particle size for acetate buffer (Canepari et al., 2010). Although the results of the previous studies may differ from those of the present study, the mechanism on the influences of particle size on the inhalation bioaccessibility of chemicals must be carefully considered.

3.5. Role of total organic carbon

To date, no studies have been conducted to assess the effects of particle size on HOCs in regards to inhalation risk, but the effects of particle size on bioaccessibility in sediments have been evaluated. In most cases, these studies have obtained similar findings as in the present study that smaller size fractions result in lower bioaccessibility (Cornelissen et al., 1999; Sun et al., 2008). However, a subset of previous studies have shown the opposite trend, *i.e.*, larger-sized sediment particles with higher TOC possess lower bioaccessibility than finer particles with lower TOC (Li et al., 1996; Wu et al., 2016). This trend is believed to be driven by TOC rather than particle size (Amweg et al., 2006). These results are significant in demonstrating the importance of chemical hydrophobicity and particle size, as well as TOC, in influencing the bioaccessibility of chemicals.

In general, higher bioaccessibility was found in lower TOC sediments (Amweg et al., 2006). The ramifications of different TOCs for differing particles, however, were not observed in the present study as each size fraction of particles contained almost the same TOC (Table 1). The similarities of TOC (31% to 38% in ALF and 33% to 48% in MGS) were attributed to the fact that these samples are from the same burning source. Although this was a drawback of the present study as it did not allow for adequate representation of e-waste particulates, it was also a strength as TOC did not affect the results, thereby allowing for a more accurate investigation of the relationship between particle size and IBAF.

It should be noted, however, that particles from burning e-waste contained quite high levels of TOC than particles from other systems. For instance, TOC contents in soil particles (Li et al., 1996) and air particles (Zhang et al., 2009) are below 5%, which is an order of magnitude lower than what was observed in the present study (up to 50%). Although the role of TOC in IBAF determination and ultimately risk characterization was not the focus of this study, the information provided here shows that further work on this topic is warranted and would be a of extreme importance when assessing inhalation health risk of HOCs associated with airborne particulate matter.

3.6. Inhalation health risk assessment based on bioaccessibility

The combined health risks for all PAHs and all size fractions (Table 2) illustrate the overall importance of evaluating these additional parameters, *i.e.*, IBAF and deposition fraction in the lung. E-waste burning particle inhalation health risk based on the total concentration ($Risk_O$) for an adult was 2.56×10^{-4} and 6.2×10^{-5}, respectively, without the incubation in ALF and MGS. This risk decreases dramatically when deposition efficiency ($Risk_{DE}$) is also considered (3.06×10^{-5} for ALF and 7.3×10^{-6} for MGS) and further decreases when both deposition efficiency and bioaccessibility are considered (1.2×10^{-5} for ALF and 2.2×10^{-6} for MGS). When each of the particle size fractions is examined separately, the more refined risks

Table 2
Average inhalation health risk (10^{-6}) based on total concentration ($Risk_O$), deposition efficiency ($Risk_{DE}$), and inhalation bioaccessibility fraction ($Risk_{BA}$) with several particle diameters. $L_{DE/O}$ (%) and $L_{DE+BA/O}$ (%) show the level of refinement for defining risk when incorporating these parameters in comparison to using the total concentration ($Risk_O$).

Particulate size diameter (μm)	ALF					MGS				
	$Risk_O$	$Risk_{DE}$	$Risk_{DE+BA}$	$L_{DE/O}$	$L_{DE+BA/O}$	$Risk_O$	$Risk_{DE}$	$Risk_{DE+BA}$	$L_{DE/O}$	$L_{DE+BA/O}$
Combined	255.8	30.6	12.3	12.0	4.8	62.0	7.3	2.24	12.0	3.6
0.056–0.18	45.8	8.7	3.3	18.9	7.2	6.7	1.2	0.36	18.2	5.4
0.18–0.32	65.0	4.6	1.8	7.1	2.8	12.9	0.9	0.23	6.9	1.8
0.32–0.56	63.7	5.3	1.1	8.2	1.7	13.2	1.1	0.18	7.9	1.4
0.56–1.0	366.3	4.7	1.6	12.8	4.4	13.6	1.7	0.32	12.4	2.4
1.0–1.8	25.4	4.4	2.5	17.3	9.8	9.0	1.5	0.58	16.7	6.4
1.8–5.6	19.6	3.0	2.0	15.6	10.2	6.5	1.0	0.59	15	9.1

($Risk_{DE}$ and $Risk_{DE+BA}$) are still much lower than 90% of $Risk_O$ (Table 2 and Fig. S5). Additionally, the IBAF trends discussed above for differing size particles, in general, hold the same pattern when assessing risk, *i.e.*, inhalation risk increased with increasing particle size. Consequently the ratio between $Risk_{DE+BA}$ and $Risk_O$ increased from the smallest to the largest fraction by up to 5.9 and 6.6 fold for ALF and MGS, respectively.

Duan et al. (2015) recently proposed that the risk-based management of PAHs should consider bioaccessibility. Our results echo this sentiment, suggesting bioaccessibility should always be favored over more traditional evaluations, such as total concentration. If contaminated sites are evaluated for inhalation health risk using total concentrations, the potential risk is substantially higher and in many cases this conclusion may be inaccurate leading to possible expensive remediation efforts. As the number of sites with possible inhalation health risk continues to rise globally (Abbas et al., 2009; Luo et al., 2014; Wu et al., 2015), being able to accurately characterize and ultimately prioritize contaminated sites is highly needed by risk assessors.

It is noteworthy that the estimated inhalation health risk only evaluated 10 individual PAHs detected (Table S3) was quite conservative, *i.e.*, the inhalation risk of particles themselves, gaseous PAHs, other possible organics or metals which would also be present in e-waste burning airborne particles has not been considered. Furthermore, the present study assumed that all particles that came into the body would make contact with the interstitial fluid within the deep lung or were phagocytized by alveolar and macrophages which would not be the case in reality. Therefore, the significance of the risk assessment conducted herein was to demonstrate the impact of bioaccessibility on the assessment outcome, but not the outcome itself. Surely, the bioaccessible fraction derived from the *in vitro* method should be further validated by future *in vivo* studies.

4. Conclusions

An *in vitro* method with MGS and ALF was developed for evaluating the inhalation bioaccessibility of particle-bound HOCs. The IBAFs of PAHs in e-waste burning particles decreased with increasing hydrophobicity, but increased with increasing particle sizes except for 4-ring PAHs in ALF. Finally, the present study suggested that the deposition efficiency and bioaccessibility of particle-bound HOCs were significant factors in the human inhalation health risk assessment.

Acknowledgements

The present study was financially supported by the National Natural Science Foundation of China (Nos. 41390240 and 21722701). We would also like to thank W. Tyler Mehler for assistance with manuscript editing.

Appendix A. Supplementary data

Supplementary data to this article can be found online at https://doi.org/10.1016/j.envint.2018.08.015.

References

Abbas, I., Saint-Georges, F., Billet, S., Verdin, A., Mulliez, P., Shirali, P., Garcon, G., 2009. Air pollution particulate matter ($PM_{2.5}$)-induced gene expression of volatile organic compound and/or polycyclic aromatic hydrocarbon-metabolizing enzymes in an in vitro coculture lung model. Toxicol. in Vitro 23, 37–46.

Amweg, E.L., Weston, D.P., You, J., Lydy, M.J., 2006. Pyrethroid insecticides and sediment toxicity in urban creeks from California and Tennessee. Environ. Sci. Technol. 40, 1700–1706.

Balakrishnan, K., Ghosh, S., Ganguli, B., Sambandam, S., Bruce, N.G., Barnes, D.F., 2014. An integrated risk function for estimating the global burden of disease attributable to ambient fine particulate matter exposure. Environ. Health Perspect. 122, 397–403.

Beelen, R., Raaschou-Nielsen, O., Stafoggia, M., Andersen, Z.J., Weinmayr, G., Hoffmann, B., Wolf, K., Samoli, E., Fischer, P., Nieuwenhuijsen, M., Vineis, P., Xun, W.W., Katsouyanni, K., Dimakopoulou, K., Oudin, A., Forsberg, B., Modig, L., Havulinna, A.S., Lanki, T., Turunen, A., Oftedal, B., Nystad, W., Nafstad, P., De Faire, U., Pedersen, N.L., Ostenson, C.G., Fratiglioni, L., Penell, J., Korek, M., Pershagen, G., Eriksen, K.T., Overvad, K., Ellermann, T., Eeftens, M., Peeters, P.H., Meliefste, K., Wang, M., Bueno-de-Mesquita, B., Sugiri, D., Kramer, U., Heinrich, J., de Hoogh, K., Key, T., Peters, A., Hampel, R., Concin, H., Nagel, G., Ineichen, A., Schaffner, E., Probst-Hensch, N., Kunzli, N., Schindler, C., Schikowski, T., Adam, M., Phuleria, H., Vilier, A., Clavel-Chapelon, F., Declercq, C., Grioni, S., Krogh, V., Tsai, M.Y., Ricceri, F., Sacerdote, C., Galassi, C., Migliore, E., Ranzi, A., Cesaroni, G., Badaloni, C., Forastiere, F., Tamayo, I., Amiano, P., Dorronsoro, M., Katsoulis, M., Trichopoulou, A., Brunekreef, B., Hoek, G., 2014. Effects of long-term exposure to air pollution on natural-cause mortality: an analysis of 22 European cohorts within the multicentre ESCAPE project. Lancet 383, 785–795.

Beriro, D.J., Cave, M.R., Wragg, J., Thomas, R., Wills, G., Evans, F., 2016. A review of the current state of the art of physiologically-based tests for measuring human dermal in vitro bioavailability of polycyclic aromatic hydrocarbons (PAH) in soil. J. Hazard. Mater. 305, 240–259.

Bernhard, W., 2016. Lung surfactant: function and composition in the context of development and respiratory physiology. Ann. Anat.-Anat. Anz. 208, 146–150.

Bevan, D.R., Yonda, N.T., 1985. In vitro technique to study elution of benzo[a]pyrene from particulates into biomembranes with application to woodstove particulates. Anal. Biochem. 150, 105–110.

Birmili, W., Allen, A.G., Bary, F., Harrison, R.M., 2006. Trace metal concentrations and water solubility in size-fractionated atmospheric particles and influence of road traffic. Environ. Sci. Technol. 40, 1144–1153.

Boisa, N., Elom, N., Dean, J.R., Deary, M.E., Bird, G., Entwistle, J.A., 2014. Development and application of an inhalation bioaccessibility method (IBM) for lead in the PM_{10} size fraction of soil. Environ. Int. 70, 132–142.

Borm, P.J.A., Cakmak, G., Jermann, E., Weishaupt, C., Kempers, P., van Schooten, F.J., Oberdorster, G., Schins, R.P.F., 2005. Formation of PAH-DNA adducts after in vivo and vitro exposure of rats and lung cells to different commercial carbon blacks. Toxicol. Appl. Pharmacol. 205, 157–167.

Canepari, S., Astolfi, M.L., Moretti, S., Curini, R., 2010. Comparison of extracting solutions for elemental fractionation in airborne particulate matter. Talanta 82, 834–844.

Choi, J.H., Ryu, J., Jeon, S., Seo, J., Yang, Y.-H., Pack, S.P., Choung, S., Jang, K.-S., 2017. In-depth compositional analysis of water-soluble and -insoluble organic substances in fine ($PM_{2.5}$) airborne particles using ultra-high-resolution 15T FT-ICR MS and GC × GC-TOFMS. Environ. Pollut. 225, 329–337.

Collins, C.D., Craggs, M., Garcia-Alcega, S., Kademoglou, K., Lowe, S., 2015. Towards a unified approach for the determination of the bioaccessibility of organic pollutants. Environ. Int. 78, 24–31.

Cornelissen, G., van Nort, P.C.M., Parsons, J.R., Govers, H.A.J., 1997. Temperature dependence of slow adsorption and desorption kinetics of organic compounds in sediments. Environ. Sci. Technol. 31, 454–460.

Cornelissen, G., Zuilen, H.v., Noort, P.C.M.v., 1999. Particle size dependence of slow

desorption of in situ PAHs from sediments. Chemosphere 38, 2369–2380.
Cui, X.Y., Xiang, P., He, R.W., Juhasz, A., Ma, L.Q., 2016. Advances in in vitro methods to evaluate oral bioaccessibility of PAHs and PBDEs in environmental matrices. Chemosphere 150, 378–389.
Dartey, E., Berlinger, B., Thomassen, Y., Ellingsen, D.G., Odland, J.O., Nartey, V.K., Yeboah, F.A., Weinbruch, S., 2014. Bioaccessibility of lead in airborne particulates from car battery repair work. Environ. Sci. Process. Impacts 16, 2782–2788.
Delfino, R., Sioutas, C., Malik, S., 2005. Potential role of ultrafine particles in associations between airborne particle mass and cardiovascular health. Environ. Health Perspect. 113, 934–946.
Duan, L.C., Naidu, R., Thavamani, P., Meaklim, J., Megharaj, M., 2015. Managing long-term polycyclic aromatic hydrocarbon contaminated soils: a risk-based approach. Environ. Sci. Pollut. Res. 22, 8927–8941.
Fang, M.L., Stapleton, H.M., 2014. Evaluating the bioaccessibility of flame retardants in house dust using an in vitro Tenax bead-assisted sorptive physiologically based method. Environ. Sci. Technol. 48, 13323–13330.
Gerde, P., Muggenburg, B.A., Lundborg, M., Dahl, A.R., 2001. The rapid alveolar absorption of diesel soot-adsorbed benzo[a]pyrene: bioavailability, metabolism and dosimetry of an inhaled particle-borne carcinogen. Carcinogenesis 22, 741–749.
Hofmann, W., Asgharian, B., 2003. The effect of lung structure on mucociliary clearance and particle retention in human and rat lungs. Toxicol. Sci. 73, 448–456.
Julien, C., Esperanza, P., Bruno, M., Alleman, L.Y., 2011. Development of an in vitro method to estimate lung bioaccessibility of metals from atmospheric particles. J. Environ. Monit. 13, 621–630.
Kademoglou, K., Giovanoulis, G., Palm-Cousins, A., Padilla-Sanchez, J.A., Magnér, J., de Wit, C.A., Collins, C.D., 2018. In vitro inhalation bioaccessibility of phthalate esters and alternative plasticizers present in indoor dust using artificial lung fluids. Environ. Sci. Technol. Lett. 5, 329–334.
Kastury, F., Smith, E., Juhasz, A.L., 2017. A critical review of approaches and limitations of inhalation bioavailability and bioaccessibility of metal(loid)s from ambient particulate matter or dust. Sci. Total Environ. 574, 1054–1074.
Kioumourtzoglou, M.A., Austin, E., Koutrakis, P., Dominici, F., Schwartz, J., Zanobetti, A., 2015. $PM_{2.5}$ and survival among older adults effect modification by particulate composition. Epidemiology 26, 321–327.
Li, J.H., Langford, C.H., Gamble, D.S., 1996. Atrazine sorption by a mineral soil: effects of soil size fractions and temperature. J. Agric. Food Chem. 44, 3680–3684.
Li, H.B., Chen, K., Juhasz, A.L., Huang, L., Ma, L.Q., 2015. Childhood lead exposure in an industrial town in China: coupling stable isotope ratios with bioaccessible lead. Environ. Sci. Technol. 49, 5080–5087.
Li, S.W., Li, H.B., Luo, J., Li, H.M., Qian, X., Liu, M.M., Bi, J., Cui, X.Y., Ma, L.Q., 2016. Influence of pollution control on lead inhalation bioaccessibility in $PM_{2.5}$: a case study of 2014 Youth Olympic Games in Nanjing. Environ. Int. 94, 69–75.
Luo, P., Bao, L.-J., Wu, F.-C., Li, S.-M., Zeng, E.Y., 2014. Health risk characterization for resident inhalation exposure to particle-bound halogenated flame retardants in a typical e-waste recycling zone. Environ. Sci. Technol. 48, 8815–8822.
Martins, V., Moreno, T., Cruz Minguillon, M., van Drooge, B.L., Reche, C., Amato, F., de Miguel, E., Capdevila, M., Centelles, S., Querol, X., 2016. Origin of inorganic and organic components of $PM_{2.5}$ in subway stations of Barcelona, Spain. Environ. Pollut. 208, 125–136.
McLachlan, M.S., 1994. Model of the fate of hydrophobic contaminants in cows. Environ. Sci. Technol. 28, 2407–2414.
Mehler, W.T., Li, H.Z., Pang, J.X., Sun, B.Q., Lydy, M.J., You, J., 2011. Bioavailability of hydrophobic organic contaminants in sediment with different particle-size distributions. Arch. Environ. Contam. Toxicol. 61, 74–82.
Pelfrêne, A., Cave, M.R., Wragg, J., Douay, F., 2017. In vitro investigations of human bioaccessibility from reference materials using simulated lung fluids. Int. J. Environ. Res. Public Health 112.
Ruby, M.V., Lowney, Y.W., 2012. Selective soil particle adherence to hands: implications for understanding oral exposure to soil contaminants. Environ. Sci. Technol. 46, 12759–12771.
Semple, K.T., Doick, K.J., Jones, K.C., Burauel, P., Craven, A., Harms, H., 2004. Defining bioavailability and bioaccessibility of contaminated soil and sediment is complicated. Environ. Sci. Technol. 38, 228a–231a.
Shen, H.T., Starr, J., Han, J.L., Zhang, L., Lu, D.S., Guan, R.F., Xu, X.M., Wang, X.F., Li, J.G., Li, W.W., Zhang, Y.J., Wu, Y.N., 2016. The bioaccessibility of polychlorinated biphenyls (PCBs) and polychlorinated dibenzo-p-dioxins/furans (PCDD/Fs) in cooked plant and animal origin foods. Environ. Int. 94, 33–42.
Sun, K., Ran, Y., Yang, Y., Xing, B., 2008. Sorption of phenanthrene by nonhydrolyzable organic matter from different size sediments. Environ. Sci. Technol. 42, 1961–1966.
Twining, J., McGlinn, P., Loi, E., Smith, K., Giere, R., 2005. Risk ranking of bioaccessible metals from fly ash dissolved in simulated lung and gut fluids. Environ. Sci. Technol. 39, 7749–7756.
Veldhuizen, E.J.A., Haagsman, H.P., 2000. Role of pulmonary surfactant components in surface film formation and dynamics. Biochim. Biophys. Acta Biomembr. 1467, 255–270.
Wei, W., Bonvallot, N., Gustafsson, A., Raffy, G., Glorennec, P., Krais, A., Ramalho, O., Le Bot, B., Mandin, C., 2018. Bioaccessibility and bioavailability of environmental semi-volatile organic compounds via inhalation: a review of methods and models. Environ. Int. 113, 202–213.
Wiseman, C.L.S., 2015. Analytical methods for assessing metal bioaccessibility in airborne particulate matter: a scoping review. Anal. Chim. Acta 877, 9–18.
Wiseman, C.L.S., Zereini, F., 2014. Characterizing metal(loid) solubility in airborne PM_{10}, $PM_{2.5}$ and PM_1 in Frankfurt, Germany using simulated lung fluids. Atmos. Environ. 89, 282–289.
Witt, E.C., Shi, H.L., Wronkiewicz, D.J., Pavlowsky, R.T., 2014. Phase partitioning and bioaccessibility of Pb in suspended dust from unsurfaced roads in Missouri-a potential tool for determining mitigation response. Atmos. Environ. 88, 90–98.
Wu, C.-C., Bao, L.-J., Guo, Y., Li, S.-M., Zeng, E.Y., 2015. Barbecue fumes: an overlooked source of health hazards in outdoor settings? Environ. Sci. Technol. 49, 10607–10615.
Wu, C.-C., Bao, L.-J., Tao, S., Zeng, E.Y., 2016. Significance of antifouling paint flakes to the distribution of dichlorodiphenyltrichloroethanes (DDTs) in estuarine sediment. Environ. Pollut. 210, 253–260.
Zereini, F., Wiseman, C.L.S., Puettmann, W., 2012. In vitro investigations of platinum, palladium, and rhodium mobility in urban airborne particulate matter (PM_{10}, $PM_{2.5}$, and PM_1) using simulated lung fluids. Environ. Sci. Technol. 46, 10326–10333.
Zhang, B.Z., Guan, Y.F., Li, S.M., Zeng, E.Y., 2009. Occurrence of polybrominated diphenyl ethers in air and precipitation of the pearl river delta, south China: annual washout ratios and depositional rates. Environ. Sci. Technol. 43, 9142–9147.
Zhang, K., Zhang, B.Z., Li, S.M., Wong, C.S., Zeng, E.Y., 2012. Calculated respiratory exposure to indoor size-fractioned polycyclic aromatic hydrocarbons in an urban environment. Sci. Total Environ. 431, 245–251.
Zhang, Y.Y., Pignatello, J.J., Tao, S., Xing, B.S., 2015. Bioaccessibility of PAHs in fuel soot assessed by an in vitro digestive model with absorptive sink: effect of food ingestion. Environ. Sci. Technol. 49, 14641–14648.
Zhang, Y., Pignatello, J.J., Tao, S., 2016. Bioaccessibility of nitro- and oxy-PAHs in fuel soot assessed by an in vitro digestive model with absorptive sink. Environ. Pollut. 218, 901–908.
Zhang, Y., Peng, M., Yu, C., Zhang, L., 2017. Burden of mortality and years of life lost due to ambient PM_{10} pollution in Wuhan, China. Environ. Pollut. 230, 1073–1080.